https://doi.org/10.1016/j.energy.2020.118117

The separation of ternary azeotropic mixture: thermodynamic insight and improved multi-objective optimization

Shirui Sun [a], Wei Chun [b], Ao Yang [a], Weifeng Shen [a,*], Peizhe Cui [c] and Jingzheng Ren [d]

[a] School of Chemistry and Chemical Engineering, Chongqing University, Chongqing 400044, PR China

[b]School of Economics and Business Administration, Chongqing University, Chongqing 400044, PR China

[c] College of Chemical Engineering, Qingdao University of Science and Technology, 53 Zhengzhou Road, Qingdao, 266042, PR China

[d] Department of Industrial and Systems Engineering, The Hong Kong Polytechnic University, Hong Kong, PR China

Corresponding Author: *(W. Shen) E-mail: shenweifeng@cqu.edu.cn

School of Chemistry and Chemical Engineering, Chongqing University, Chongqing 400044, PR China

Abstract： Acetonitrile (ACN) and Ethanol (EtOH) are important organic solvents and they are frequently used as mobile phase in high performance liquid chromatography resulting in the production of waste ternary mixture ACN/EtOH/water. The separation of such ternary systems is a key to recovery valuable solvents in waste liquid from views on economic and environmental benefits. Thus, we proposed an effective separation strategy of triple-column extractive distillation (TCED) to separate such ternary mixture with three binary azeotropes and a single ternary azeotrope for the first time. The suitable entrainer and the separation sequence were determined by thermodynamic insights (*i.e.,* residue curve maps, isovolatility line, univolatility line and material balance lines). In addition, an improved multi-objective genetic algorithm optimization embedding the weak mutation and detection/deduplication of overlapping solutions was employed to optimize the proposed process with plenty of continuous and discrete decision variables. Finally, DMSO was determined as the most appropriate entrainer to separate such complex ternary mixture. The separation sequence of TCED process was determined as the ACN first, then EtOH and water as the last product. The optimal TCED process with the trade-off benefits between fixed capital investment and annual operating costs was obtained.

Keywords: Ternary azeotropic mixture; Conceptual design; Triple-column extractive distillation; Multi-objective optimization

1 Introduction

Acetonitrile (ACN) and Ethanol (EtOH) are frequently applied as an mobile phase

in high performance liquid chromatography, which causes the production of ACN/EtOH/water mixture [1]. Moreover, such ternary mixture also generates in the production process of ACN by dehydrogenation of ethanol and ammonia [2]. Therefore, the recovery of ACN and EtOH from the wastewater should be investigated to achieve sustainable development. Unfortunately, such ternary mixture is a complex system with three binary azeotropes and a single ternary azeotrope at atmospheric pressure indicating the separation of such ternary system is difficult.

It is generally known that extractive distillation (ED) [3] and [4], pressure-swing distillation [5-7], azeotropic distillation [8] and [9] are usually used to realize the separation of azeotropic mixtures. The development of ED process has attracted considerable attentions from both industry and academia due to the advantages in low energy consumption and easy recycling of entrainers [10]. For instance, an ED process with indirect sequence for separating methanol and toluene *via* intermediate-boiling solvent trimethylamine was proposed to reduce solvent recycle flowrates and energy requirements [11]. Zhang *et al.* [12] investigated the determination of the best entrainer in ED process *via* the isovolatility curve. Ma *et al.* [13] explored the design, optimization and control of ED process *via* ionic liquid (*i.e.,* 1-ethyl-3-methylimidazolium dicyanamide) to separate isopropanol-water.

The separation of binary azeotropic mixture by ED process has been extensively investigated. The separation of ACN-EtOH binary azeotropic mixture can be achieved by ED process using 1-butyl-3-methylimidazolium dibutyl-phosphate as entrainer [14].

Yang *et al.* [6] reported an extractive pressure-swing distillation to separate binary azeotropic mixture dimethyl carbonate and EtOH. Shang *et al.* [15] proposed an ED process for the separation of EtOH/water mixture using deep eutectic solvent as entrainer. However, more complex mixture (*e.g.,* ternary azeotropes and ternary mixture with multi-azeotropes) will generate in the actual chemical industry. Hence, the investigation for separating such complex mixture *via* energy-saving ED process is necessary.

On the other hand, some studies on process optimization were carried out to save more energy consumptions in chemical and petroleum industries [16-18]. Zhang *et al.* [19] optimized an ED process for separation of the mixture ethyl-acetate/EtOH by a sequential iterative optimization procedure. However, sequential iterative method is not able to provide decent optimization of complex chemical processes with a large amount of nonlinear continuous and discrete decision variables. A multi-objective genetic algorithm in MATLAB is used for the optimization of the ED for ACN/water to minimize the total cost under purity constraints [20], and the results demonstrated that the optimal design shows the energy consumption and TAC reduced by more than 20% than the referenced case.

So far, the separation strategy of ACN/EtOH/water ternary mixture with a single ternary azeotrope and three binary azeotropes has not been found in the reported studies. In this work, a preliminary conceptual design indicates that the separation of such complex ternary system could be achieved to obtain more economic and environmental

benefits. Hereby, the contribution of this study is focused on the following three aspects: the first one is that we proposed an effective triple-column extractive distillation (TCED) process to separate such ternary mixture with a ternary and three binary azeotropes for the first time. Second, the suitable entrainer and the separation sequence of proposed TCED process for such multi-azeotrope mixture were determined *via* the thermodynamic insights combining residue curve maps, isovolatility line, univolatility line and material balance lines. Third, an improved multi-objective genetic algorithm optimization embedding the weak mutation and detection/deduplication of overlapping solutions was applied to the proposed TCED process to obtain optimal design variables.

2 Methodology

A systematic procedure for thermodynamic insights and improved multi-objective optimization of ternary systems ACN/EtOH/water with a ternary and three binary azeotropes through TCED process is shown in Figure 1. In the first step, the best entrainer for separating such mixture should be determined among candidate entrainer (*i.e.,* NMP, DMSO and glycerol) *via* the comparison of isovolatility and univolatility lines. After that, the separation sequence and thermodynamic feasibility of the proposed TCED process is analyzed *via* conceptual design combining residue curve maps and material balance lines. Finally, the proposed TCED process is optimized *via* the improved multi-objective genetic algorithm based on the trade-off between fixed capital investment and annual operating costs.

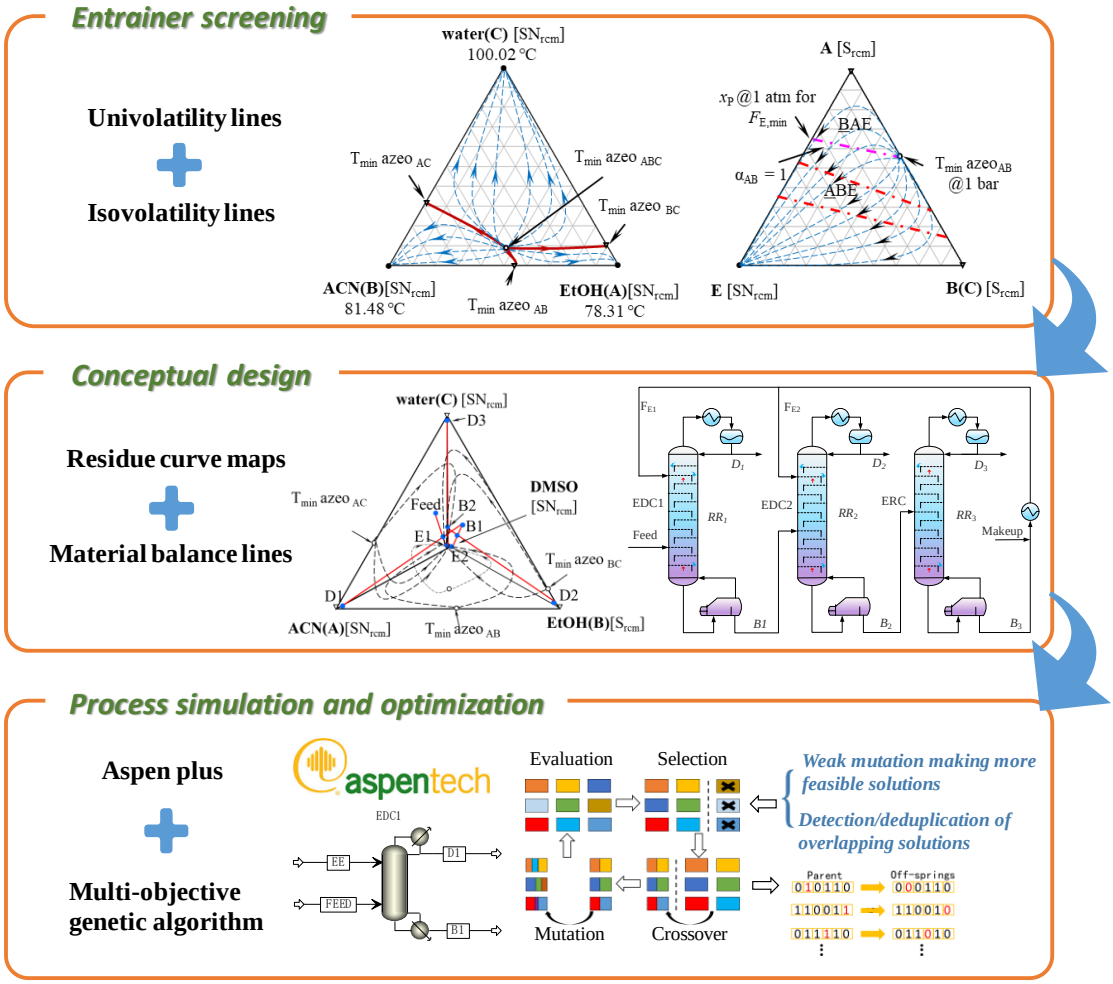

Figure 1 Proposed procedure based on the thermodynamic insight and improved multi-objective genetic algorithm for complex mixture ACN/EtOH/water

2.1 Thermodynamic insight

In this study, ACN/EtOH/water ternary mixture with three binary azeotropes (*i.e.,* ACN/EtOH, ACN/water, EtOH/water) and a ternary azeotrope (*i.e.,* ACN/EtOH/water) belongs to class 3.1-2 of Serafimov's classification (shown in Figure 2(a)) [21]. As is evident that there is a distillation boundary dividing the residue curve maps into three regions causing the separation of such mixture to be more difficult. Figure 2(b) presents the univolatility, isovolatility curve and the residue curve maps of binary azeotropes (A-B, A-C, or B-C) with a heavy entrainer (E). From the observation of Figure 2(b),

the univolatility curve divides the ternary diagram (ABE) into two regions and the volatility orders of the top and bottom region are BAE and ABE, respectively. The azeotrope of A-B can be broke in the feasibility region ABE and the component A could be obtained at the distillate stream *via* a direct extractive distillation column when the flow rate of entrainer is larger than the minimum value.

For the ED process, the suitable entrainer indicates high separation efficiency and low energy consumption [22]. The intersection point between univolatility curve and binary side A-E is called as the x_P which can be used to evaluate the capability of entrainer [23] and [24]. The closer the intersection to target component (*i.e.*, small value of x_P), the less the amount of entrainer is employed. Similarly, the closer intersection point between isovolatility curve and binary side A-E indicates higher separation efficiency and lower energy costs.

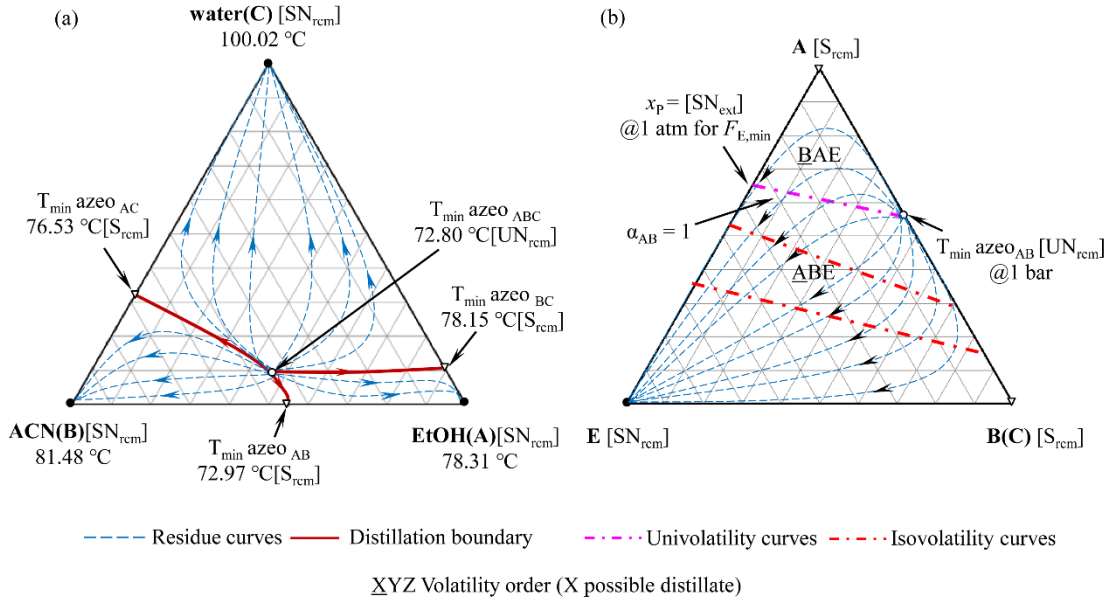

Figure 2. (a) Residue curve maps of ACN/EtOH/water (b) Topological features and univolatility lines for binary azeotropic mixture with a heavy entrainer (E) at 1.0 atm

The residue curve maps and material balance lines can be used for the conceptual design and the determination of separation sequence. The material balance lines of distillation process are represented by straight lines in the residue curve maps and overall flow rates are based on the inverse-lever-arm rule. It is worth noting that there are two constraints for material balance lines. On the one hand, the bottoms, distillate and overall feed compositions should be collinear. On the other hand, the distillate and bottoms product must lie on the same residue curve.

2.2 Process simulation and optimization

Thermodynamic model

The accuracy of the steady-state simulation depends on the selection of the thermodynamic model [25] and [26]. According to property method selection assistant in Aspen Plus, the activity coefficient methods (e.g., NRTL, WILSON, UNIQUAC and UNIFAC) can be used to describe the vapor-liquid equilibrium behavior of the highly non-ideal ternary mixture ACN/EtOH/water. However, the binary interaction parameters between ACN and DMSO for WILSON and UNIQUAC are missing.

For making a choice between NRTL and UNIFAC, we compare the x-y diagrams prediction values with those of experimental data as shown in Figure S1 of Supporting Information, which indicates that the vapor-liquid equilibria of (a) EtOH and water, (b) EtOH and ACN, (c) water and ACN, (d) EtOH and DMSO, and (e) water and DMSO predicted by NRTL and UNIFAC are both consistent with the experimental data [27-31]. However, as shown in Figure S1(f), the vapor-liquid equilibrium of ACN and

DMSO predicted by NRTL has more predominate advantage than UNIFAC as compared to the experimental data [32]. As such, the thermodynamic model NRTL is chosen to describe the vapor-liquid equilibrium behavior in this work. All binary interaction parameters are provided in Table 1. The ACN/EtOH/water mixture are frequently used as mobile phase in high performance liquid chromatography resulting in the generation of wastewater and the feed flow rate is set to 100 kmol/h with the composition of 45.3 mol% ACN, 13.1 mol% EtOH, and 41.6 mol% water [1]. The purities of three products ACN, EtOH and water are all specified as 99.9 mol%.

Table 1 NRTL binary interaction parameters for ACN/EtOH/water

Component *i*	EtOH	EtOH	Water	EtOH	Water	ACN
Component *j*	Water	ACN	ACN	DMSO	DMSO	DMSO
Temperature units	°C	°C	°C	°C	°C	°C
Source	APV84 VLE-IG	APV84 VLE-IG	APV84 VLE-IG	APV84 VLE-IG	APV84 VLE-IG	NISTV84 NIST-HOC
a_{ij}	-0.8009	-0.5982	1.0567	0.0000	-1.2449	0.1056
a_{ji}	3.4578	-0.9745	-0.1164	0.0000	1.7524	1.7296
b_{ij}	246.18	478.02	283.41	116.54	586.80	-2.6506
b_{ji}	-586.08	435.76	256.46	-393.32	-1130.2	76.186

Multi-objective genetic algorithm optimization

Herein, an improved multi-objective genetic algorithm is applied to optimize the proposed TCED process to provide quantitative trade-off between annual operation cost and fixed capital investment. The improved multi-objective genetic algorithm procedure includes generation of initial population, simulation, external storage of Pareto-optimal solution, generation of off-springs and end (see Figure 3). There are two measures to improve the existing non-dominated sorting genetic algorithm: the first one

is the deduplication of the overlapping individuals from the merged population before the non-dominant sorting, and another one is weak mutation that aims to ensure that more feasible solution could be obtained and the overall search direction is not changed substantially (denoted as purple square frames in Figure 3). It is noteworthy that the connection between the improved multi-objective genetic algorithm based on VB.NET and Aspen Plus is achieved by Active X [33]. This optimization procedure will find improved individuals throughout the generations and generate a set of the Pareto-front that moving towards the optimal solutions.

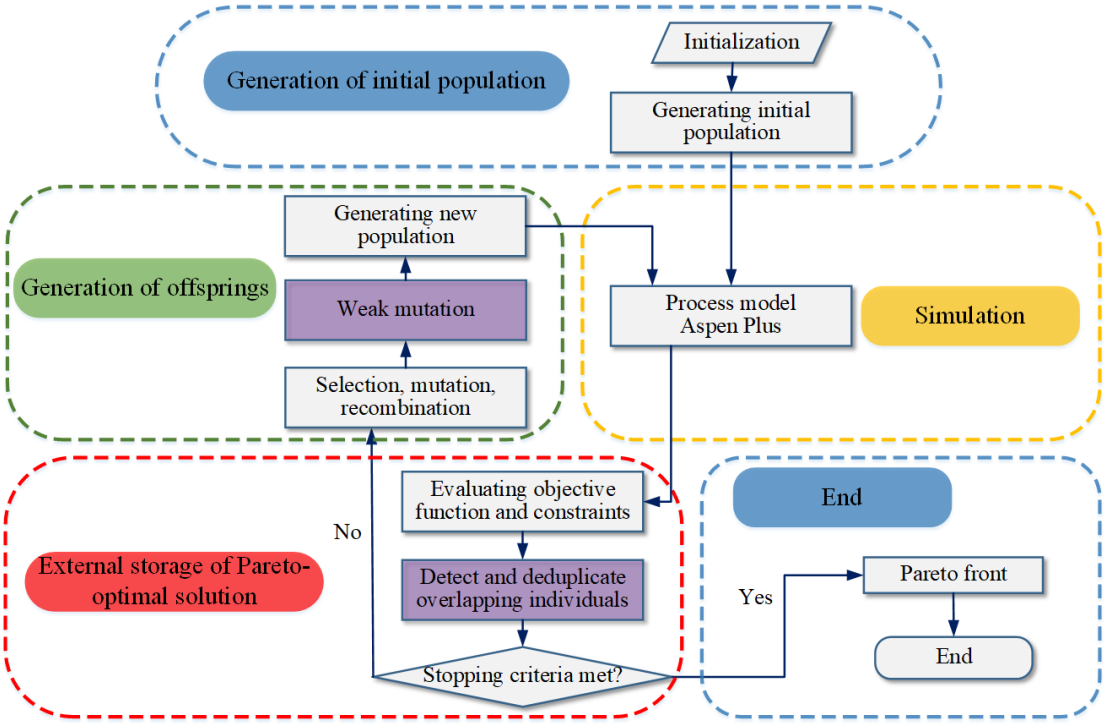

Figure 3 The multi-objective genetic algorithm optimization procedure for the TCED process

Objective Function

The design of ED is frequently evaluated through introducing objective function TAC (denoted as Equation1) to find the optimal design variables, which is typically defined in single-objective optimization [34] and [35].

$$TAC = \frac{FCI}{Payback\ period} + AOC \tag{1}$$

In fact, TAC consists of annual operation cost and fixed capital investment. Herein, fixed capital investment is the sum of capital costs of columns, trays, condensers, and reboilers while the costs of pipes, pumps, and valves and the subsequent wastewater treatment cost are neglected [36]; the annual operation cost includes the annual costs of steam and cooling water [37] and [38]. In the design of chemical process, fixed capital investment and annual operation cost are two conflicting objectives indicating that higher equipment investments would cause more savings in annual operation cost. Thus, minimizing both fixed capital investment and annual operation cost are chosen as objective functions in this study, and the detail calculation of annual operation cost and fixed capital investment are presented in Table 2. The Tray Sizing function in Aspen Plus is employed to size the column diameter *d*.

Table 2. Basis of economics and equipment sizing

column height (h): N_T trays with 2 ft spacing plus 20% extra length
column and other vessel (d and h are in meters)
$capital\ cost\ (\$) = \left(\frac{M\&S}{280}\right) \times 937.64 \times d_{col}^{1.006} \times h_{col}^{0.802} \times (2.18+3.67)$
column Tray (d and h are in meters)
$capital\ cost\ (\$) = \left(\frac{M\&S}{280}\right) \times 97.24 \times d^{1.55} \times h_{tray} \times (1.0+1.7)$
reboilers (area in m^2)
heat-transfer coefficient = 0.568 kW/K·m^2
differential temperature = steam temperature − base temperature
$capital\ cost\ (\$) = \left(\frac{M\&S}{280}\right) \times 474.67 \times A^{0.65} \times 7.35$
coolers (area in m^2)
heat-transfer coefficient = 0.852 kW/K·m^2
differential temperature = [a]LMTD of inlet and outlet temperature
$capital\ cost\ (\$) = \left(\frac{M\&S}{280}\right) \times 474.67 \times A^{0.65} \times 5.29$
energy cost
low pressure steam = \$7.78/GJ (5 bar, 433.15 K)

medium pressure steam = $8.22/GJ (10 bar, 457.15 K)
high pressure steam = $9.88/GJ (41 bar, 527.15K)
cooling water (315K) = $0.354/GJ
[a]LMTD: logarithmic mean temperature difference.

Decision variables

There are several decision variables, consisting of eight discrete variables (*i.e.*, the total stage numbers and feed stages of EDC1, EDC2 and ERC and the entrainer feed stages of EDC1 and EDC2) and eight continuous variables (the reflux ratios and distillate rates of EDC1, EDC2 and ERC and the flowrate and split ratio of entrainer), need to be optimized. An initial trial of MOGA is performed to determine the bounds on decision variables. The generation number and population size of the initial trial were set as 50 and 20 because larger generation number and population size would lead to long computational times [39].

The results show that the fixed capital investment and annual operating costs drastically decrease with the reduction of the reflux ratios and flowrate of entrainer indicating the lower bounds of those decision variables need to be as low as possible. The lower total stage numbers of EDC1, EDC2 and ERC lead to higher reflux ratio and energy consumptions indicating that the total stage numbers of those column should be less than 20. And the entrainer should be fed at the top section of EDC1 and EDC2. Thus, the initial trial can narrow the bounds on decision variable to reduce the computational effort and time. The lower and upper bounds of some key decision variables are therefore obtained as shown in Table 3.

Table 3 The lower and upper bounds of key decision variables in TCED

Decision variable	Units	Lower bound	Upper bound

NT1		20	45
NT2		20	45
NT3		20	45
NF1		5	35
NFE1		2	9
NF2		5	35
NFE2		2	9
NF3		5	35
RR1		0.1	10
RR2		0.1	10
RR3		0.1	10
FSE1		0.1	1
EE	kmol/h	100	300
D1	kmol/h	45.3	45.9
D2	kmol/h	13.1	13.2
D3	kmol/h	41.6	41.7

Constraints

Desired product purities are respectively defined in Equations (2)-(5), which are executed as constraint functions in the multi-objective genetic algorithm procedure.

$$x_{ACN} \geq 99.9 \text{ mol\%} \quad (2)$$

$$x_{EtOH} \geq 99.9 \text{ mol\%} \quad (3)$$

$$x_{water} \geq 99.9 \text{ mol\%} \quad (4)$$

$$x_{Entrainer} \geq 99.9 \text{ mol\%} \quad (5)$$

The size of population, crossover factors and mutation factors are set as 100, 0.90 and 0.15, respectively [20]. And the overall optimization procedure is carried out on a 64 bit desktop computer with an Intel Core i7-6700HQ CPU @ 2.60 GHz, including an 8 GB RAM.

3 Results and discussion

3.1 Thermodynamic insight results

In this work, the promising entrainers DMSO, NMP and glycerol are selected as candidate entrainers for separating ACN/EtOH/water mixture. As shown in Figure S2 of Supporting Information, the residue curve maps of possible binary mixtures with glycerol indicate that glycerol could make such ternary system more complex due to the existing of heterogeneous region. In addition, the boiling point of glycerol is 287.71℃ indicating the entrainer recovery column must operate under vacuum condition to ensure adequate heat transfer temperature difference of reboiler increasing the fixed capital investments. Thus, glycerol is an inappropriate entrainer from the economic perspective.

The isovolatility and univolatility lines at 1.00 atm for six ternary systems consists of possible binary mixtures with DMSO and NMP (*i.e.*, ACN/EtOH/DMSO, ACN/water/DMSO, EtOH/water/DMSO, ACN/EtOH//NMP, ACN/water/NMP, and EtOH/water/NMP) are shown in Figure 4. From the comparison of the intersection between one target component (*i.e.*, ACN, ACN and EtOH in Figure 4(a)-(b), 4(c)-(d) and 4(e)-(f), respectively) and univolatility curves, the results demonstrate that DMSO is a better entrainer than NMP for separating ACN/EtOH/water mixture. On the other hand, the intersection between target component and isovolatility of DMSO is also small than that of NMP indicating that DMSO is superior to NMP in enhancing relative volatility of three azeotropes. Therefore, the entrainer DMSO is finally applied to the separation of ACN/EtOH/water mixtures.

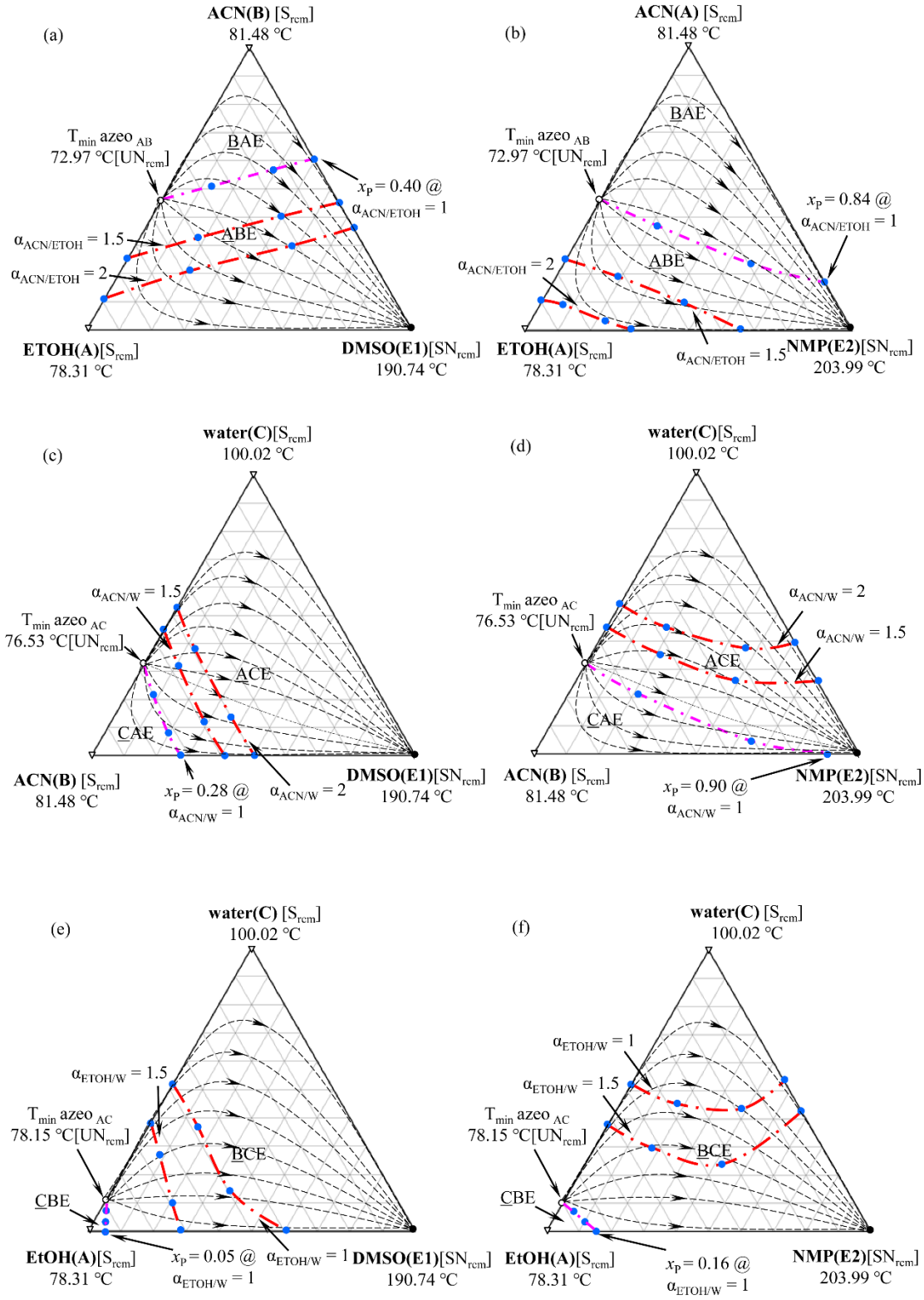

Figure 4 Isovolatility and univolatility lines at 1.0 atm for (a), (b) ACN/EtOH, (c), (d) ACN/water, and (d), (f) EtOH/water using entrainer DMSO and NMP, respectively

The residue curve maps and material balance lines for separating the

ACN/EtOH/water mixture using TCED are illustrated in Fig 5(a) and the TCED process including two extractive distillation columns (*i.e.*, EDC1 and EDC2) and an entrainer-recovery column (*i.e.*, ERC) is presented in Figure 5(b). In this process, fresh feed ACN/EtOH/water mixture (*i.e.*, Feed) and entrainer (*i.e.*, E1) respectively enter the top and bottom section of EDC1 to maintain adequate mass transfer. In EDC1, ACN (*i.e.*, D1) moves toward the top of EDC1 while EtOH/water mixture with DMSO (*i.e.*, B1) moves toward the bottom of EDC1 because the entrainer can alter the relative volatility of ACN/EtOH and ACN/water. The bottom stream of EDC1 (*i.e.*, B1) and another part of the entrainer (*i.e.*, E2) are sent to EDC1 for separating EtOH and water. Similarly, DMSO alters the relative volatility between EtOH and water causing EtOH (*i.e.*, D2) moves toward the top part and water with DMSO (*i.e.*, B2) moves toward the bottom part of EDC2. The bottom stream of EDC2 (*i.e.*, B2) is fed into ERC to produce water in the distillate (*i.e.*, D3) and entrainer in the column bottom (*i.e.*, E). DMSO is recycled back to EDC1 and EDC2. To balance the tiny entrainer losses in three distillates, the makeup stream of entrainer is added. The optimal feed locations (*i.e.*, NFE1, NFE2, NF1, NF2, and NF3), reflux ratios (*i.e.*, RR1, RR2, and RR3), and entrainer flow rates (FE1 and FE2) are obtained by the following optimization section.

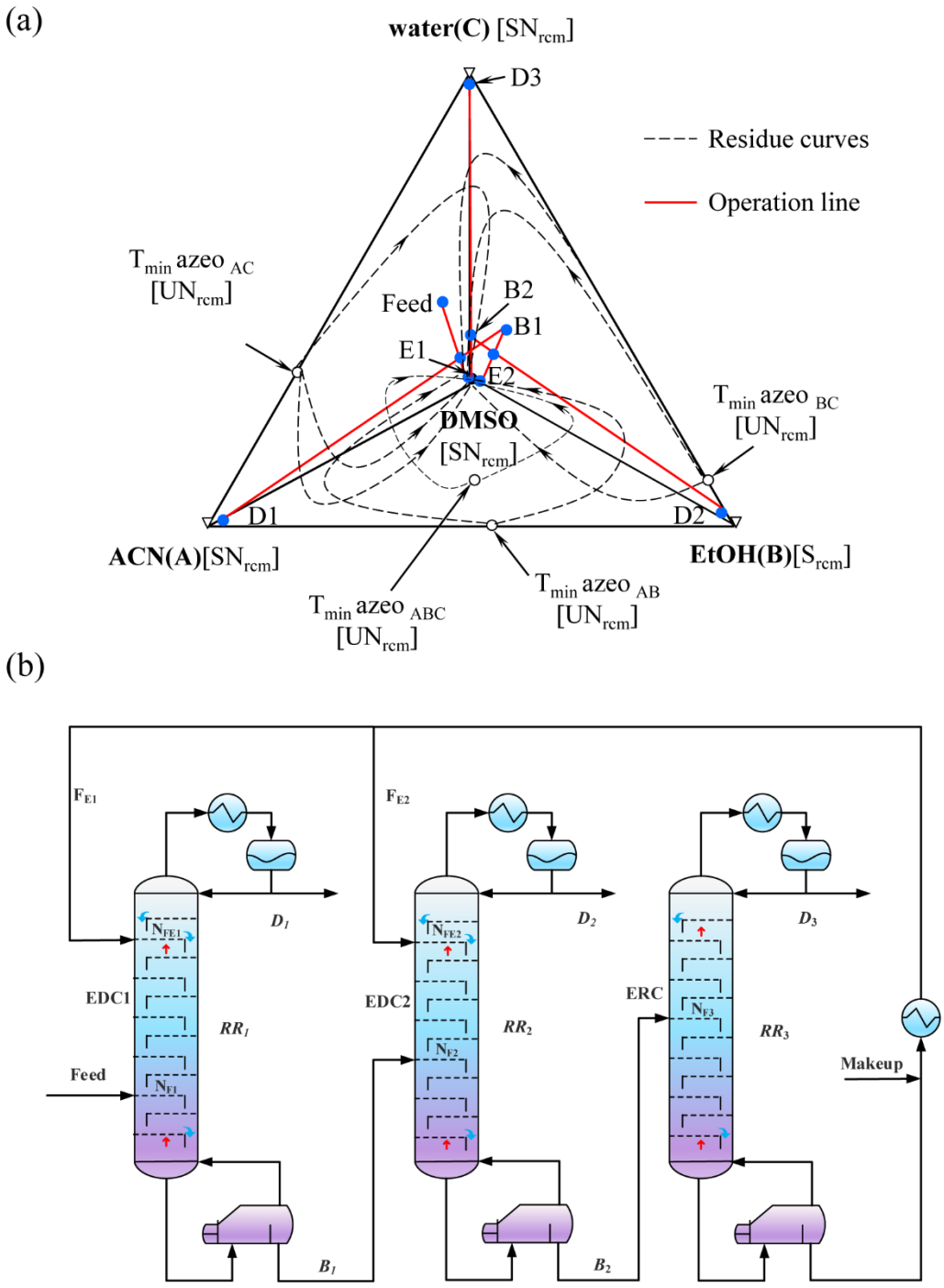

Figure 5 (a) material balance lines for separating ACN/EtOH/water using TED, (b) conceptual design flowsheet of TCED

3.2 Optimization results

In this work, the multi-objective genetic algorithm procedure took about 154 hours to get the optimization results. Figure 6 shows the final Pareto-optimal front solutions

and the evolution process of the Pareto-optimal solutions for the TCED optimization. The intermediate solutions of Pareto-optimal front at interval of 200 generations are presented to confirm the termination of multi-objective genetic algorithm procedure. As depicted in the inset of Figure 6, there is a slight improvement in respective Pareto fronts of the objective functions from 1100th to 1300th generation. The iteration could be stopped when the generational distance is very close to zero [40]. As such, the optimization is stopped at the end of 1300 generations whose generational distance is 0.0003. The solution of multi-objective optimization is not unique because single solution cannot satisfy the competing objectives at the same time [41]. A set of Pareto-optimal front in 1300th generation is shown in the main plot of Figure 6, and it can be observed that fixed capital investment ranges from 1.255 to 1.271 million $ and annual operation cost from 0.785 to 0.801 million $/year. It is noteworthy that the Pareto-optimal front has two discontinuities due to the existing of discrete characteristic of the optimization variables (*i.e.*, total stage numbers and feed stages of EDC1, EDC2 and ERC).

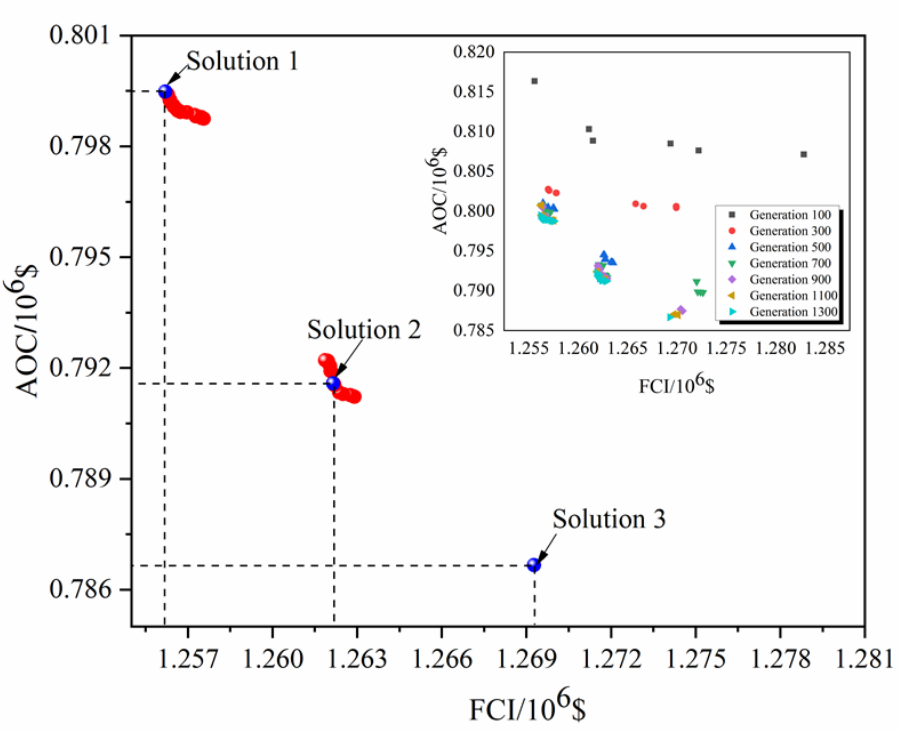

Figure 6 Pareto-optimal front (main plot) and intermediate solutions (inset) for the TCED process

Once obtained the Pareto optimal set, the decision maker can choose an optimal solution according to the best trade-offs between fixed capital investment and annual operation cost. Three solutions of interested studied designs (shown in blue filled marker in Figure 6) are listed in Table 4. The uppermost left blue marker in Figure 7 (Solution 1), corresponds to the solution with lowest fixed capital investment (1.256 million $) and highest annual operation cost (0.799 million $), whereas the downmost right blue marker in Figure 7 (Solution 3) is the highest fixed capital investment (1.269 million $) solution and lowest annual operation cost (0.787 million $) supplied. Thus, fixed capital investment and annual operation cost are mutually competitive relationship. The total stage numbers of EDC1, the reflux ratio of ERC (RR3) and the flowrate of entrainer are the key design variables in such TCED process and the effects of such design variables on fixed capital investment and annual operating costs are

shown in Figure S3 of Supporting Information. For the lower annual operating costs, the reflux ratio of ERC and the flowrate of entrainer need to be lower (shown in Figure S3(b) and (c) of Supporting Information). On the other hand, both lower the reflux ratio of ERC and the flowrate of entrainer require higher total stage numbers of EDC1 to keep higher separation efficiency causing the higher fixed capital investment (shown in Figure S3(a) of Supporting Information). Therefore, the contradictory relationship of design variables leads to the competitive relationship of fixed capital investment and annual operating costs. Following the suggestion of Alcocer-García et al. [42], Solution 2 is considered as the optimal design by weighing fixed capital investment and annual operating costs.

Table 4 Design parameters and performance indexes for the TCED process

	Solution 1	Solution 2	Solution 3
NT1	37	35	34
NT2	45	45	45
NT3	20	20	20
NFE1	7	7	7
NFE2	4	4	4
NF1	26	26	26
NF2	23	23	24
NF3	7	7	7
D1	45.3390	45.3354	45.3324
D2	13.1000	13.1000	13.1000
D3	41.6039	41.6033	41.6039
RR1	0.2099	0.2103	0.2097
RR2	2.3965	2.3964	2.3963
RR3	0.9179	0.9250	0.9486
EE	171.93	174.55	177.70
FSE1	0.6454	0.6448	0.6440
FCI (10^6\$)	1.2693	1.2622	1.2562
AOC(10^6\$/y)	0.7866	0.7916	0.7995
TAC(10^6\$/y)	1.2098	1.2122	1.2182

Optimal flowsheet of TCED process for separating ACN/EtOH/water system using entrainer DMSO is illustrated in Figure 7. The total numbers of stages of EDC1, EDC2 and ERC are 35, 45 and 20, respectively. The optimized feed location of EDC1, EDC2 and ERC are 26th, 23th and 7th stages, respectively. Besides, entrainer are fed at 7th and 4th stages in EDC1 and EDC2, respectively. The optimized RR1, RR2, RR3 and total flow rates of entrainer (EE) are 0.2103, 2.3964, 0.9250 and 174.55 kmol/h, respectively. An entrainer makeup (*i.e.*, 0.0400 kmol/h) is added to balance the tiny entrainer losses in three distillates. Simultaneously, the obtained optimized distillate rates D1, D2 and D3 of EDC1, EDC2 and ERC are 45.3354, 13.1000 and 41.6033 kmol/h, respectively.

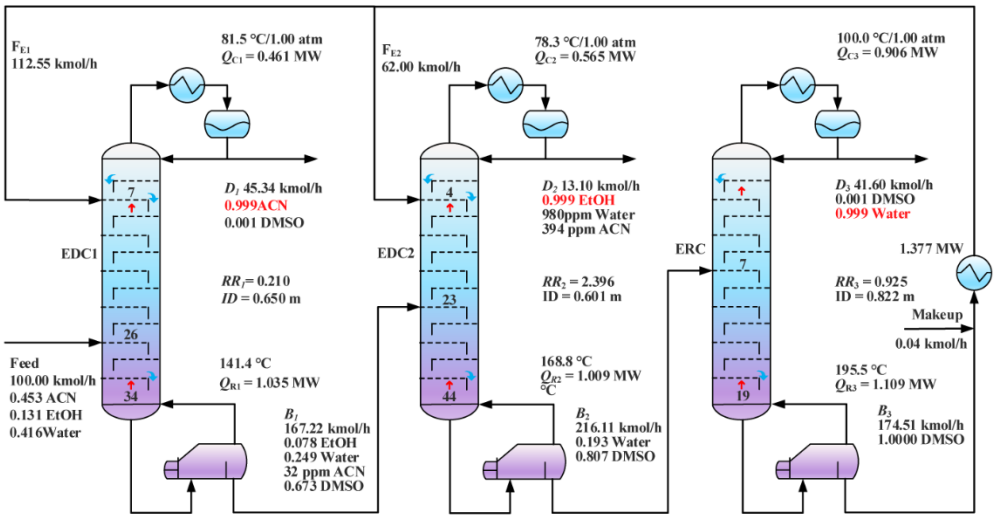

Figure 7 Optimal TCED process for separating ACN/EtOH/water system using entrainer DMSO

Figure 8 illustrates the liquid composition and temperature profiles in columns EDC1, EDC2 and ERC. The ACN composition (marked as pink circle in Figure 8(a)) increases drastically from 7th stage to 1st stage due to the azeotrope breaking and high purity of ACN with 99.9 mol% is eventually obtained at 1st stage. The EtOH

composition (marked as red circle in Figure 8(c)) increases drastically from 4th stage to 1st stage and high purity of EtOH with 99.9 mol% eventually achieves at 1st stage. In addition, the water composition achieves its highest purity of 99.9 mol% at stage 1 of ERC (see Figure 8(e)).

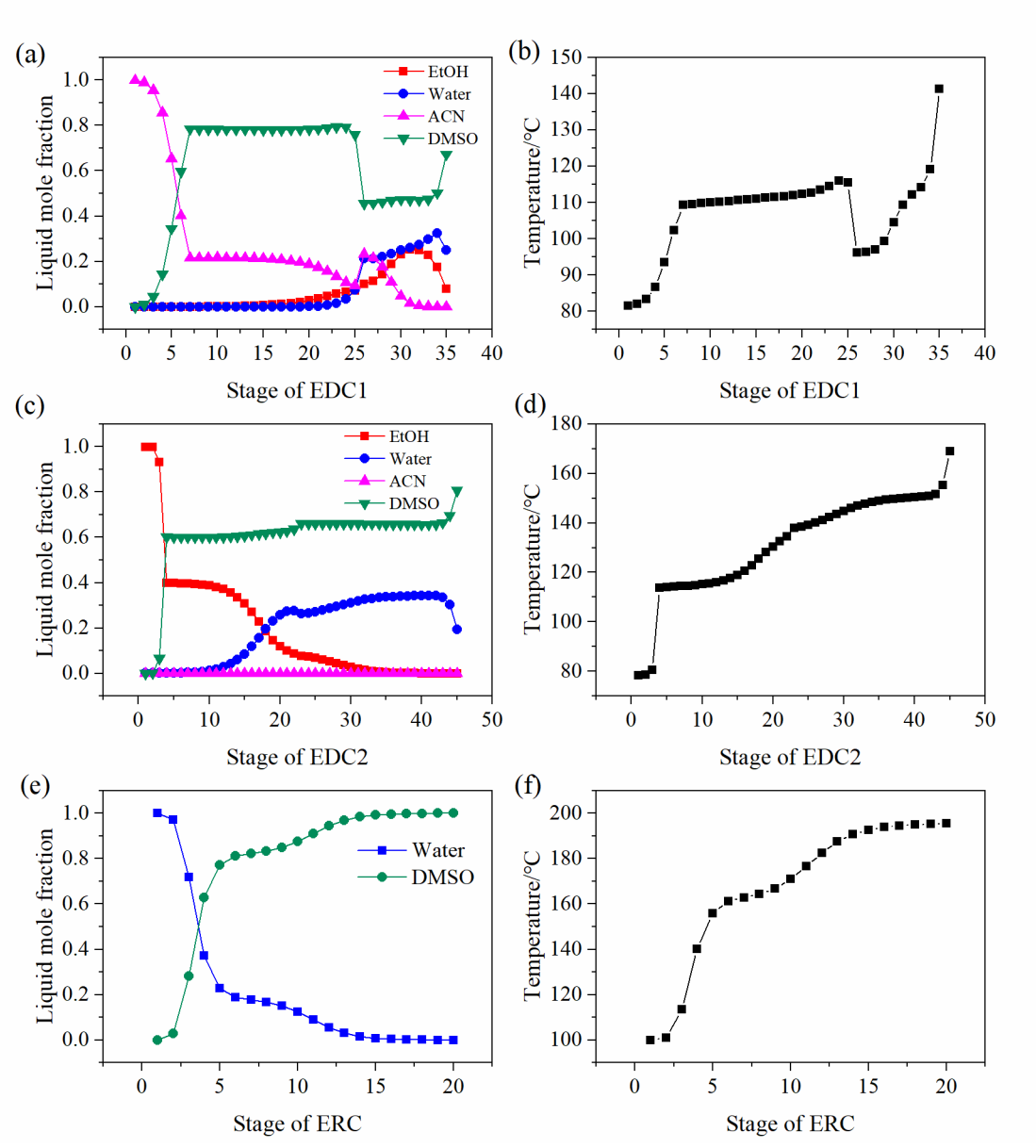

Figure 8. Liquid composition and temperature profiles in (a), (b) EDC1, (c), (d) EDC2 and (e), (f) ERC

4 Conclusions

In this work, an efficient strategy through the triple-column extractive distillation

(TCED) for separating Acetonitrile (ACN)/Ethanol (EtOH)/water with a single ternary and three binary azeotropes was proposed to obtain more economic and environmental benefits. Based on the results of thermodynamic insight and improved optimization, the following conclusions can be drawn:

(1) DMSO was determined as the most suitable entrainer *via* the univolatility and isovolatility lines;

(2) The conceptual design of the TCED process was designed *via* the combination of residue curve maps and material balance lines. The separation sequence of TCED process was determined as the ACN first, then EtOH and water as the last product while the products would be distillated from the top of three columns EDC1, EDC2 and ERC, respectively;

(3) The optimal design of TCED process with the trade-off benefits between fixed capital investment and annual operating costs was obtained *via* an improved multi-objective genetic algorithm embedding the weak mutation and the detection/deduplication of overlapping solutions.

It is worth to mention that the proposed systematic approach can be widely extended to the separation of other similar ternary mixtures with multi-azeotrope. Moreover, robust control strategies such as dual-temperature control and composition control can be further explored to investigate the dynamic controllability of such TCED process.

Acknowledgments

We acknowledge the financial support provided by the National Natural Science Foundation of China (No. 21606026, 21878028); the Fundamental Research Funds for the Central Universities (No. 106112019CDQYHG021).

Nomenclature

ACN	acetonitrile
EtOH	ethanol
TCED	triple-column extractive distillation
ED	extractive distillation
NMP	n-methyl pyrrolidone
DMSO	dimethyl sulfoxide
TAC	total annual cost, US$/y
FCI	fixed capital investment, US$
AOC	annual operation cost, US$/y
A	area, m^2
EDC1	extractive distillation column 1
EDC2	extractive distillation column 2
ERC	entrainer recycle column
NT1-3	total number of stages of columns EDC1, EDC2 and ERC
NF1-3	feed locations of columns EDC1, EDC2 and ERC
NFE1	feed locations of entrainer in EDC1
NFE2	feed locations of entrainer in EDC2

D1-3 distillate rates of columns EDC1, EDC2 and ERC, kmol/h

RR1-3 reflux ratios of columns EDC1, EDC2 and ERC

FE flowrate of entrainer, kmol/h

FSE1 split fraction of entrainer into EDC1

ID_{1-3} diameter of columns C1-C3, m

References

[1] Thurmann S, Belder D. Phase-optimized chip-based liquid chromatography. Anal Bioanal Chem. 2014;406(26):6599-606.

[2] Brown KW, Donnelly KC. Mutagenic activity of the liquid waste from the production of acetonitrile. Bulletin of Environmental Contamination and Toxicology. 1984;32(1):742-8.

[3] Yang A, Zou H, Chien IL, Wang D, Wei S, Ren J, et al. Optimal Design and Effective Control of Triple-Column Extractive Distillation for Separating Ethyl Acetate/Ethanol/Water with Multiazeotrope. Industrial & Engineering Chemistry Research. 2019;58(17):7265-83.

[4] Sun S, Lü L, Yang A, Wei S, Shen W. Extractive distillation: Advances in conceptual design, solvent selection, and separation strategies. Chinese Journal of Chemical Engineering. 2019;27(6):1247-56.

[5] Yang A, Shen W, Wei S, Dong L, Li J, Gerbaud V. Design and control of pressure-swing distillation for separating ternary systems with three binary minimum azeotropes. AIChE Journal. 2019;65(4):1281-93.

[6] Yang A, Sun S, Shi T, Xu D, Ren J, Shen W. Energy-efficient extractive pressure-swing distillation for separating binary minimum azeotropic mixture dimethyl carbonate and ethanol. Separation and Purification Technology. 2019;229:115817.

[7] Liang S, Cao Y, Liu X, Li X, Zhao Y, Wang Y, et al. Insight into pressure-swing distillation from azeotropic phenomenon to dynamic control. Chemical Engineering Research and Design. 2017;117:318-35.

[8] Chen J, Ye Q, Liu T, Xia H, Feng S. Improving the performance of heterogeneous azeotropic distillation via self-heat recuperation technology. Chemical Engineering Research and Design. 2019;141:516-28.

[9] Yang A, Jin S, Shen W, Cui P, Chien IL, Ren J. Investigation of energy-saving azeotropic dividing wall column to achieve cleaner production via heat exchanger network and heat pump technique. Journal of Cleaner Production. 2019;234:410-22.

[10] Hu Y, Su Y, Jin S, Chien IL, Shen W. Systematic approach for screening organic and ionic liquid solvents in homogeneous extractive distillation exemplified by the tert-butanol dehydration. Separation and Purification Technology. 2019;211:723-37.

[11] Luyben WL. Improved design of an extractive distillation system with an intermediate-boiling solvent. Separation and Purification Technology. 2015;156:336-47.

[12] Zhang X, Li X, Li G, Zhu Z, Wang Y, Xu D. Determination of an optimum entrainer for extractive distillation based on an isovolatility curve at different pressures. Separation and Purification Technology. 2018;201:79-95.

[13] Ma S, Shang X, Zhu M, Li J, Sun L. Design, optimization and control of extractive distillation for the separation of isopropanol-water using ionic liquids. Separation and Purification Technology. 2019;209:833-50.

[14] Zhang Z, Zhang D, Li W, Zhang T, Wu K, Yang R, et al. Separation of acetonitrile + ethanol mixture using imidazolium - Based ionic liquids as entrainers. Fluid Phase Equilibria. 2018;474:43-9.

[15] Shang X, Ma S, Pan Q, Li J, Sun Y, Ji K, et al. Process analysis of extractive distillation for the separation of ethanol–water using deep eutectic solvent as entrainer. Chemical Engineering Research and Design. 2019;148:298-311.

[16] Rangaiah GP, Bonilla-Petriciolet A. Multi-Objective Optimization in Chemical Engineering: Developments and Applications, John Wiley & Sons, Ltd, New York, 2013

[17] Wang Y, Bu G, Geng X, et al. Design optimization and operating pressure effects in the separation of acetonitrile/methanol/water mixture by ternary extractive distillation. Journal of cleaner production, 2019, 218: 212-224.

[18] Primabudi E, Morosuk T, Tsatsaronis G. Multi-objective optimization of propane pre-cooled mixed refrigerant (C3MR) LNG process. Energy. 2019;185:492-504.

[19] Zhang Q, Liu M, Li C, Zeng A. Design and control of extractive distillation process for separation of the minimum-boiling azeotrope ethyl-acetate and ethanol. Chemical Engineering Research and Design. 2018;136:57-70.

[20] You X, Gu J, Gerbaud V, Peng C, Liu H. Optimization of pre-concentration, entrainer recycle and pressure selection for the extractive distillation of acetonitrile-water with ethylene glycol. Chemical Engineering Science. 2018;177:354-68.

[21] Kiva VN, Hilmen EK, Skogestad S. Azeotropic phase equilibrium diagrams: a survey. Chemical Engineering Science. 2003;58(10):1903-53.

[22] Shen W, Dong L, Wei S, Li J, Benyounes H, You X, et al. Systematic design of an extractive distillation for maximum-boiling azeotropes with heavy entrainers. AIChE Journal. 2015;61(11):3898-910.

[23] Shen W, Gerbaud V. Extension of thermodynamic insights on batch extractive distillation to continuous operation. 2. azeotropic mixtures with a light entrainer. Industrial & Engineering Chemistry Research. 2013;52(12):4623-37.

[24] Shen W, Benyounes H, Gerbaud V. Extension of thermodynamic insights on batch extractive distillation to continuous operation. 1. azeotropic mixtures with a heavy entrainer. Industrial & Engineering Chemistry Research. 2013;52(12):4606-22.

[25] Wang Z, Su Y, Shen W, Jin S, Clark JH, Ren J, et al. Predictive deep learning

models for environmental properties: the direct calculation of octanol–water partition coefficients from molecular graphs. Green Chemistry. 2019;21(16):4555-65.

[26] Su Y, Wang Z, Jin S, Shen W, Ren J, Eden MR. An Architecture of Deep Learning in QSPR Modeling for the Prediction of Critical Properties Using Molecular Signatures. AIChE Journal. 2019;65(9):e16678.

[27] Kamihama N, Matsuda H, Kurihara K, Tochigi K, Oba S. Isobaric vapor–liquid equilibria for ethanol+ water+ ethylene glycol and its constituent three binary systems. Journal of Chemical & Engineering Data. 2012;57(2):339-44.

[28] Dohnal V, Veselý F, Holub R, Pick J. Liquid-vapour equilibrium and heats of mixing in the ethanol-acetonitrile system. Collection of Czechoslovak Chemical Communications. 1982;47(12):3177-87.

[29] Acosta J, Arce A, Rodil E, Soto A. A thermodynamic study on binary and ternary mixtures of acetonitrile, water and butyl acetate. Fluid Phase Equilibria. 2002;203(1):83-98.

[30] Kaczmarek B, Radecki A. Vapor-liquid equilibria in binary systems containing ethanol with hexamethyldisiloxane and dimethyl sulfoxide. Journal of Chemical & Engineering Data. 1989;34(2):195-7.

[31] Peng Y, Ping L, Lu S, Mao J. Vapor–liquid equilibria for water+ acetic acid+(N, N-dimethylformamide or dimethyl sulfoxide) at 13.33 kPa. Fluid Phase Equilibria. 2009;275(1):27-32.

[32] Wang Q, Zeng H, Song H, Liu Q, Yao S. Vapor− Liquid Equilibria for the Ternary System Acetonitrile+ 1-Propanol+ Dimethyl Sulfoxide and the Corresponding Binary Systems at 101.3 kPa. Journal of Chemical & Engineering Data. 2010;55(11):5271-5.

[33] Su Y, Jin S, Zhang X, Shen W, Eden MR, Ren J. Stakeholder-oriented multi-objective process optimization based on an improved genetic algorithm. Computers & Chemical Engineering. 2020;132:106618.

[34] Douglas JM. Conceptual design of chemical processes: McGraw-Hill New York, 1988.

[35] Wang C, Zhuang Y, Liu L, et al. Design and control of a novel side-stream extractive distillation column for separating methanol-toluene binary azeotrope with intermediate boiling entrainer. Separation and Purification Technology, 2020;239:116581.

[36] Yang A, Su Y, Chien IL, Jin S, Yan C, Wei S, et al. Investigation of an energy-saving double-thermally coupled extractive distillation for separating ternary system benzene/toluene/cyclohexane. Energy. 2019;186:115756.

[37] Sun S, Yang A, Chien IL, Shen W, Wei S, Ren J, et al. Intensification and performance assessment for synthesis of 2-methoxy-2-methyl-heptane through the combined use of different pressure thermally coupled reactive distillation and heat integration technique. Chemical Engineering and Processing - Process Intensification. 2019;142:107561

[38] Yang A, Sun S, Eslamimanesh A, Wei S, Shen W. Energy-saving investigation

for diethyl carbonate synthesis through the reactive dividing wall column combining the vapor recompression heat pump or different pressure thermally coupled technique. Energy. 2019;172:320-32.

[39] Radatz H, Schröder M, Becker C, Bramsiepe C, Schembecker G. Selection of equipment modules for a flexible modular production plant by a multi-objective evolutionary algorithm. Computers & Chemical Engineering. 2019;123:196-221.

[40] Kumar M, Guria C. The elitist non-dominated sorting genetic algorithm with inheritance (i-NSGA-II) and its jumping gene adaptations for multi-objective optimization. Information Sciences. 2017;382-383:15-37.

[41] Beyrami J, Chitsaz A, Parham K, Arild Ø. Optimum performance of a single effect desalination unit integrated with a SOFC system by multi-objective thermo-economic optimization based on genetic algorithm. Energy. 2019;186:115811.

[42] Alcocer-García H, Segovia-Hernández JG, Prado-Rubio OA, Sánchez-Ramírez E, Quiroz-Ramírez JJ. Multi-objective optimization of intensified processes for the purification of levulinic acid involving economic and environmental objectives. Chemical Engineering and Processing - Process Intensification. 2019;136:123-37.